

UC Berkeley

UC Berkeley Previously Published Works

Title

Recovery of Forest Structure Following Large-Scale Windthrows in the Northwestern Amazon

Permalink

<https://escholarship.org/uc/item/232461hb>

Journal

Forests, 12(6)

ISSN

1999-4907

Authors

Muñoz, J David Urquiza

Marra, Daniel Magnabosco

Negrón-Juarez, Robinson I

et al.

Publication Date

2021




DOI

10.3390/f12060667

Peer reviewed

## Article

# Recovery of Forest Structure Following Large-Scale Windthrows in the Northwestern Amazon

J. David Urquiza Muñoz <sup>1,2,3,\*</sup> , Daniel Magnabosco Marra <sup>1,4</sup>, Robinson I. Negrón-Juarez <sup>5</sup> , Rodil Tello-Espinoza <sup>3</sup>, Waldemar Alegría-Muñoz <sup>3</sup>, Tedi Pacheco-Gómez <sup>3</sup>, Sami W. Rifai <sup>6</sup>, Jeffrey Q. Chambers <sup>5</sup>, Hillary S. Jenkins <sup>7</sup>, Alexander Brenning <sup>2</sup>  and Susan E. Trumbore <sup>1</sup>

- <sup>1</sup> Biogeochemical Processes Department, Max Planck Institute for Biogeochemistry, 07745 Jena, Germany; dmarra@bgc-jena.mpg.de (D.M.M.); trumbore@bgc-jena.mpg.de (S.E.T.)
- <sup>2</sup> Department of Geography, Friedrich Schiller University Jena, 07743 Jena, Germany; alexander.brenning@uni-jena.de
- <sup>3</sup> Faculty of Forestry Science, National University of the Peruvian Amazon, Iquitos 16002, Peru; rodil.tello@unapiquitos.edu.pe (R.T.-E.); waldemar.alegria@unapiquitos.edu.pe (W.A.-M.); tedi.pacheco@unapiquitos.edu.pe (T.P.-G.)
- <sup>4</sup> Forest Management Laboratory, Brazilian Institute for Amazon Research, Manaus 69060-001, AM, Brazil
- <sup>5</sup> Lawrence Berkeley National Laboratory, Berkeley, CA 94720, USA; robinson.inj@lbl.gov (R.I.N.-J.); jchambers@lbl.gov (J.Q.C.)
- <sup>6</sup> ARC Centre of Excellence for Climate Extremes, University of New South Wales, Sydney 2052, Australia; s.rifai@unsw.edu.au
- <sup>7</sup> Department of Environmental Studies, University of Redlands, Redlands, CA 92373, USA; hillary\_jenkins@redlands.edu
- \* Correspondence: jurquiza@bgc-jena.mpg.de



**Citation:** Urquiza Muñoz, J.D.; Magnabosco Marra, D.; Negrón-Juarez, R.L.; Tello-Espinoza, R.; Alegría-Muñoz, W.; Pacheco-Gómez, T.; Rifai, S.W.; Chambers, J.Q.; Jenkins, H.S.; Brenning, A.; et al. Recovery of Forest Structure Following Large-Scale Windthrows in the Northwestern Amazon. *Forests* **2021**, *12*, 667. <https://doi.org/10.3390/f12060667>

Academic Editors: Jean-Claude Rue and Barry Gardiner

Received: 20 March 2021

Accepted: 21 May 2021

Published: 25 May 2021

**Publisher's Note:** MDPI stays neutral with regard to jurisdictional claims in published maps and institutional affiliations.



**Copyright:** © 2021 by the authors. Licensee MDPI, Basel, Switzerland. This article is an open access article distributed under the terms and conditions of the Creative Commons Attribution (CC BY) license (<https://creativecommons.org/licenses/by/4.0/>).

**Abstract:** The dynamics of forest recovery after windthrows (i.e., broken or uprooted trees by wind) are poorly understood in tropical forests. The Northwestern Amazon (NWA) is characterized by a higher occurrence of windthrows, greater rainfall, and higher annual tree mortality rates (~2%) than the Central Amazon (CA). We combined forest inventory data from three sites in the Iquitos region of Peru, with recovery periods spanning 2, 12, and 22 years following windthrow events. Study sites and sampling areas were selected by assessing the windthrow severity using remote sensing. At each site, we recorded all trees with a diameter at breast height (DBH)  $\geq 10$  cm along transects, capturing the range of windthrow severity from old-growth to highly disturbed (mortality > 60%) forest. Across all damage classes, tree density and basal area recovered to >90% of the old-growth values after 20 years. Aboveground biomass (AGB) in old-growth forest was 380 ( $\pm 156$ ) Mg ha<sup>-1</sup>. In extremely disturbed areas, AGB was still reduced to 163 ( $\pm 68$ ) Mg ha<sup>-1</sup> after 2 years and 323 ( $\pm 139$ ) Mg ha<sup>-1</sup> after 12 years. This recovery rate is ~50% faster than that reported for Central Amazon forests. The faster recovery of forest structure in our study region may be a function of its higher productivity and adaptability to more frequent and severe windthrows. These varying rates of recovery highlight the importance of extreme wind and rainfall on shaping gradients of forest structure in the Amazon, and the different vulnerabilities of these forests to natural disturbances whose severity and frequency are being altered by climate change.

**Keywords:** forest blowdowns; forest succession and dynamics; natural disturbances; tree mortality; biomass

## 1. Introduction

Windthrows are associated with strong downdrafts produced during severe convective storms [1–4]. In the Amazon, windthrows are a frequent natural disturbance that influences regional tree mortality and has the potential to regulate regional biomass/carbon stocks and balance [5–10]. The geographic distribution of windthrows generally follows the pattern of rainfall across the Amazon Basin, though there are large variations in the size

and frequency of occurrence [7,11,12]. Windthrows are more frequent in the Northwestern Amazon than in the Central Amazon [12].

Windthrows create changes in forest composition and forest dynamics [13,14]. Consequently, windthrows provide niches for maintaining a diverse cohort of species [6,8,15,16]. In old-growth tropical forests, species with limited competition strategies are eventually eliminated from the community [17]. Therefore, understanding the drivers of structural and compositional change in tropical forests is important for predicting the future composition of these ecosystems [18,19], especially since the frequency and intensity of convective storms are being affected by climate change [7,12]. This knowledge is crucial for better planning initiatives of forest management and climate adaptation [20]. Numerous studies have examined the impacts of climate variability [21,22], soils, nutrient availability, geomorphological variation [23], hydrological regimes [24,25], and productivity [26] on forest structure and dynamics, but the effects of large-scale windthrows have received less attention and remain unassessed for most of the Amazon. Research in the Central Amazon has demonstrated that the recovery of biomass and functional composition depends on the size and severity of the disturbance [5,8,27]. Understanding how wind disturbances impact standing biomass and influence subsequent succession through tree establishment, growth, and mortality is an enduring task in forest ecology [28].

In this study, we investigate rates of forest recovery from windthrows in the Northwestern Amazon. We compare our results with a similar study carried out in the Central Amazon, which is characterized by a lower frequency of windthrows, poorer soils and slower turnover rates than our study region. We address the following questions: (a) Which forest structural attributes are most affected following windthrows? and (b) How rapidly do these attributes recover to old-growth conditions? This is the first assessment of forest recovery after windthrow events in the Northwestern Amazon, and provides insight into the different regional patterns of forest dynamics and vulnerability to natural disturbances.

## 2. Materials and Methods

### 2.1. Study Area

The study area is located within ~50 km of Iquitos, Peru, in a region covered with old-growth lowland forest (no flooded areas and less than 500 m a.s.l.) (Figure 1). Iquitos is characterized by its lack of dry season (no consecutive months with rainfall  $\leq 100$  mm) [29]. The mean annual rainfall is 3000 mm, and mean annual temperature is 25.9 °C. Precipitation is lowest from June to August with a mean and standard deviation of 183 mm and  $\pm 10$  mm month<sup>-1</sup>, respectively [12]. The study sites are managed by the National University of the Peruvian Amazon (UNAP). Because we want to study the timing of recovery after windthrow disturbances of differing severity, we identified a chronosequence of study sites that were affected by windthrow disturbances at different times in the past. The old-growth forests at the study sites have similar climatic, edaphic and floristic compositions. None of our study sites have experienced any major, recent or direct human impacts such as logging.

Windthrow events were identified via Landsat imagery using changes in non-photosynthetic vegetation (NPV) between sequential years [3,30]. This revealed that disturbances at the three study sites (Nauta, Napo and Oroza), occurred in a chronosequence of 2, 12 and 22 years, respectively, prior to transect installation. Oroza (named after the closest town) was windthrown in 1988, has a disturbed area of 662 ha and was surveyed in 2010 (i.e., 22 years after windthrow). Napo experienced a windthrow event in 1998, has a disturbed area of 188 ha, and was also surveyed in 2010 (12 years after windthrow). The windthrow in Nauta occurred in 2009. This site has a disturbed area of 189 ha and was surveyed in 2011 (2 years after windthrow).

Given that a chronosequence study substitutes space for time [8,31], our study sites are not strictly replicates, and there are differences in forest structure in the undisturbed parts of the transects. We acknowledge that additional temporal measurements would be needed to assess the degree to which this influences our results, and we have, in most

cases, normalized our data to the respective undisturbed forest when making comparisons across sites.

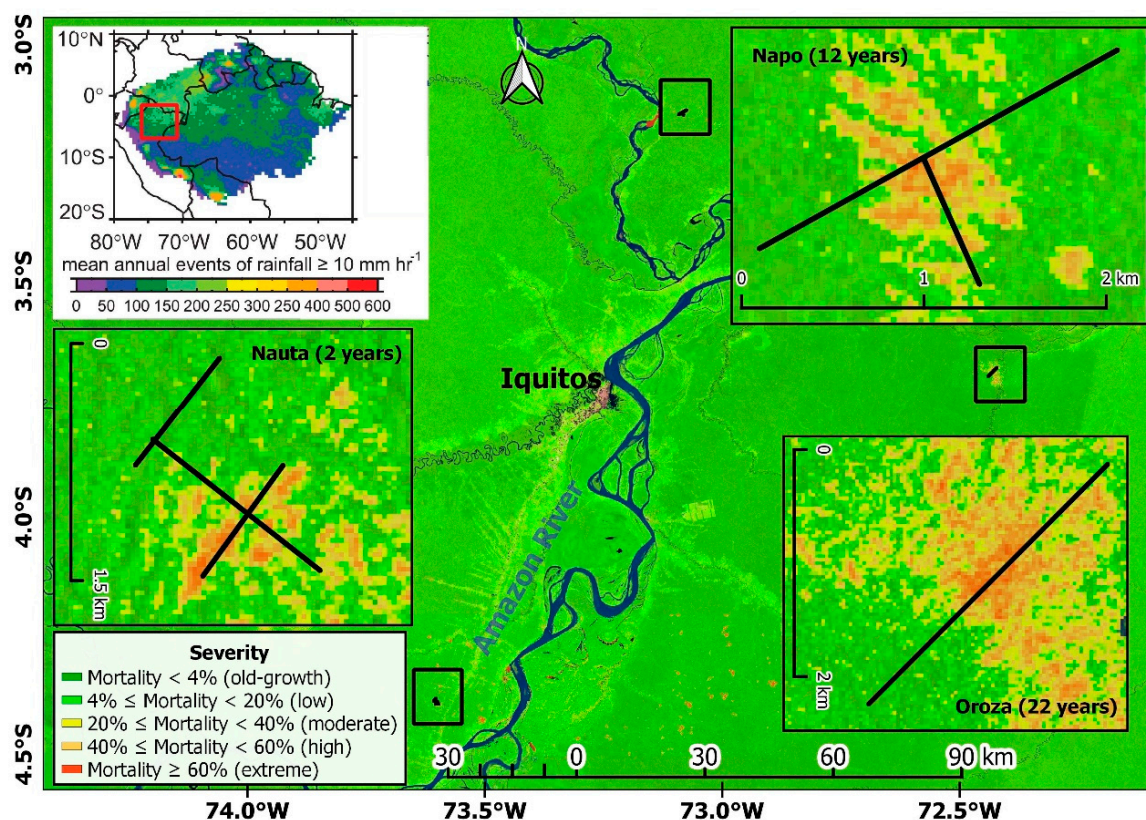


**Figure 1.** Top left inset: Map demonstrating the mean annual number of rainfall events for the period 1998–2016 obtained using TRMM. The red square indicates the location of the study sites near Iquitos, Perú. Main figure: Map of windthrow severity over the study region. Small black squares indicate the locations of the Nauta, Napo, and Oroza sites (3 ha each). These sites are enlarged in the top right, bottom right, and bottom left inset panels which include transects (black lines) located across the windthrow gradient within each field site.

## 2.2. Assessing Windthrow Severity

Landsat 5 TM images processed with LEDAPS (Landsat Ecosystem Disturbance Adaptive Processing System) [32] were used to detect the occurrence of windthrows. For Oroza, Landsat image P063R03 from 17 April 1988 (prior to disturbance) and 24 September 1988 (after disturbance) were used; for Napo, P062R03 from 19 August 1998 and 22 October 1998; and for Nauta, P063R03 from 2 September 2009 and 7 December 2009. Landsat 5 imagery with Ecosystem Disturbance Adaptive Processing System (LEDAPS) is available in the Google Earth Engine <https://earthengine.google.com>, (accessed on 24 February 2020) [33], which is the platform used for our imagery analysis and Landsat imagery processing. Windthrows were identified by their spectral characteristics (endmembers) and their distinctive shape diverging from a central area with radiant corridors separated by forest [1]. We used spectral mixture analysis (SMA) [34] to quantify the fraction of distinct endmembers. Specifically, we used image-derived endmembers: green photosynthetic vegetation (GV), non-photosynthetic vegetation (NPV), and shadows. The fractions of NPV and GV were then normalized without shadows as  $NPV/(GV + NPV)$  and  $GV/(GV + NPV)$  [3,30,34]. Metrics of the windthrow area and damage are derived from  $\Delta NPV$  [3,6,15,30,35].



Using the  $\Delta$ NPV, we estimated the percentage of trees directly toppled or killed in the studied windthrows by using a locally adjusted predictive windthrow tree-mortality model (Equation (1)) [12]:

$$M(\text{mortality, in \%}) = 99.86 \cdot \Delta\text{NPV} \quad (1)$$

To assign the mortality value by subplot ( $10 \times 30$  m), we resampled the image at a greater spatial resolution (from  $30 \times 30$  m to  $3 \times 3$  m), and extracted weighted  $\Delta$ NPV values based on the pixels comprising subplots using the Zonal statistics tool available in QGIS 3.10.3. The  $\Delta$ NPV values were used to classify windthrow severity at the subplot level, complementing previous studies in the CA [8].

### 2.3. Forest Inventory

At each site, we installed 10 m wide transects of varying lengths, with a total area of three hectares for Napo and Oroza, and 3.09 ha for Nauta. In Napo and Oroza, the transects were subdivided into 100 subplots of  $300 \text{ m}^2$  each (i.e.,  $30 \text{ m} \times 10 \text{ m}$ ), and 103 subplots for Nauta, yielding a total of 303 subplots for our analysis. The transects encompassed the entire gradient of windthrow tree-mortality derived from our remote-sensing metric [6,12]. In each subplot we measured the diameter of trees  $> 10$  cm DBH (diameter at breast height, 1.3 m). Combining all sites, we recorded 4889 living trees. A botanical sample was collected from each recorded species for tree identification. A summary of forest floristics characteristics by severity is shown in Appendix A. Tree locations were determined using a local reference system (UTM 18S) and the following procedure. First, a handheld GPS receiver (Global Position System, Garmin Map76 CSx, Olathe, Kansas, U.S.A) was used to locate the start point of each transect, then the “x” and “y” coordinates of each tree were measured using a rangefinder laser (Trimble Laserace 1000, Sunnyvale, CA, USA) based on their distance and angle from the transect’s starting position.

### 2.4. Data Processing and Analysis

The basal area (BA) of recorded trees  $\text{m}^2 \text{ ha}^{-1}$  was estimated from the diameter at breast height assuming a circular trunk shape [36]. As there are no locally adjusted allometries, we estimated individual tree aboveground biomass (AGB) using references from other Amazon regions (Models 1, 2 and 3, Table 1). The AGB at the subplot level was calculated by summing the individual biomass of trees recorded in each subplot.

**Table 1.** Allometric equations used for AGB estimation.

Model	Equation	Reference
Model 1	$\text{AGB}_{\text{est}} = \exp [-1.803 - 0.97 E + 0.976 \ln (\text{WD}) + 2.673 \ln (\text{D}) - 0.229 [\ln (\text{D})]^2]$	Equation (7) in [37]
Model 2	$\text{AGB}_{\text{est}} = 0.230 \text{D}^{2.406} \cdot (\text{WD})^{0.88}$	Equation (33) in [5]
Model 3	$\text{AGB}_{\text{est}} = 0.183 \text{D}^{2.328}$	Equation (13) in [5]

D = diameter (cm), WD = wood density ( $\text{g}/\text{cm}^3$ ), E = environmental stress.

Since Models 1 and 2 include wood density as a predictor, we compiled wood density values of recorded species from previous studies conducted in the Amazon Basin [5,8,38]. Values were assigned using data at the species, genus, or family level (in order of preference), depending on the availability and geographical proximity of our study region. Model 3 was applied to individual trees from species for which wood density was not reported.

Forest structural attributes such as biomass can be over- and/or underestimated due to spatial variations in small plots containing relatively large individual trees [5,6,39]. Previous studies from the Central Amazon suggest that robust estimates of biomass require sample units with areas between 0.08 ha to 0.12 ha [8,39]. Therefore, to reduce intrinsic

spatial variations in biomass estimates, we binned subplots from our study sites based on their windthrow severity. The final area of our binned plots ranged between 0.09–0.12 ha.

### 2.5. Statistical Analysis

A chi-square test at the 5% significance level was used to compare the diameter distribution of trees in old-growth plots. A Student's *t*-test was used to assess whether differences in mean DBH, basal area, and average AGB were statistically significant between disturbed and old-growth forest. To compare tree size, basal area, and AGB among successional stages, we used a one-way ANOVA. For reporting forest recovery, we assumed a 10% uncertainty around the respective undisturbed reference, i.e., a subplot was considered 'recovered' if it attained 90% of the old-growth value for a given attribute. We estimated the time required to recover old-growth levels of basal area and AGB by fitting linear regressions to the subplot-level data using the time since windthrow as the predictor. We further calculated 90% confidence bands of the response in order to visualize uncertainties. Although our high number of subplots (total of 303) allows for calculating confidence intervals and *p*-values independent of data distribution, these may be overly optimistic as they do not account for site-level autocorrelation. The statistical analyses were carried out in the statistical software package R 4.0.3 [40].

## 3. Results

### 3.1. Subplot Distribution by Disturbance Severity Class

Estimates of windthrow tree-mortality (Equation (1)) and the locations of transects at respective sites allowed us to calculate the number of plots and the area occupied by each severity class (Table 2). These classes encompass the range of disturbance severity from old-growth forest to low, moderate, high, and extreme severity, and are given in Table 2.

**Table 2.** The number of subplots and their total area (ha) for each windthrow tree-mortality category (defined as % of individuals) and disturbance severity class. Subplot data are given across the three study sites and periods of time (year) since windthrow.

Mortality (%)	Disturbance Severity	Years Since Windthrow			Total Number of Subplots by Severity
		2 Years	12 Years	22 Years	
≤4	Old-growth	39 (1.17 ha)	46 (1.38 ha)	35 (1.03 ha)	120
>4 & ≤20	Low	27 (0.81 ha)	20 (0.6 ha)	17 (0.51 ha)	64
>20 & ≤40	Moderate	14 (0.42 ha)	14 (0.42 ha)	7 (0.21 ha)	35
>40 & ≤60	High	10 (0.30 ha)	7 (0.21 ha)	15 (0.45 ha)	32
>60 (max:94)	Extreme	13 (0.39 ha)	13 (0.39 ha)	26 (0.78 ha)	52
Total subplots by years		103	100	100	303

### 3.2. Structural Attributes of Old-Growth Forests

Old-growth forest subplots at our study sites had a mean ( $\pm$  standard deviation) trees per hectare (TPH) of  $562 \pm 87$  trees ha<sup>-1</sup>, BA of  $24.8 \pm 2.3$  m<sup>2</sup> ha<sup>-1</sup> and AGB of  $380 \pm 156$  Mg ha<sup>-1</sup>. We assessed possible pre-disturbance differences among old-growth forests by assessing the mean diameter of trees, the basal area and the AGB across old-growth plots. The results of the ANOVA indicated a significant difference in forest structure among the study sites for BA ( $p = 0.003$ ) and AGB ( $p = 0.002$ ), but no significant differences for mean DBH ( $p = 0.079$ ). A post-hoc T-test ( $p$ -adjust using the Benjamin–Hochberg method) indicated that there is no statistical evidence of differences in mean DBH ( $p = 0.31$ ), BA ( $p = 0.55$ ), and AGB ( $p = 0.71$ ) at the Napo and Nauta sites. The Oroza site showed significant differences from the Napo site for BA ( $p = 0.02$ ) but no difference from the Nauta site ( $p = 0.06$ ). For AGB, Oroza was significantly different from Nauta and Napo ( $p = 0.007$  and  $p = 0.004$ , respectively). For mean DBH, Oroza did not differ significantly from Napo ( $p = 0.07$ ) or Nauta ( $p = 0.3$ ).

### 3.3. Recovery Patterns of Structural Attributes

#### 3.3.1. Mean Diameter, Tree Density and Basal Area

We did not find significant differences in the size distribution of trees recorded at varying windthrow severities. However, mean DBH was significantly reduced in extremely disturbed plots 2 years after windthrow ( $t$ -test  $p = 0.03$ ), but differences were not significant 12 years ( $t$ -test  $p = 0.1$ ) and 22 years ( $t$ -test  $p = 0.16$ ) after windthrow. We therefore suggest that in extremely disturbed areas, DBH has recovered to old-growth levels by year 12. For moderate and high severities, no significant differences were observed 22 years after windthrow, with  $t$ -test values of  $p = 0.58$  and  $p = 0.50$ , respectively.

The three sites, spanning 2 to 22 years after disturbance, show clear recovery of structural attributes in the decades following the respective windthrow events. Figure 2a shows the number of trees per hectare as a function of windthrow severity and recovery time. Two years after windthrow disturbance, the number of trees per hectare was  $382 (\pm 35)$  trees  $\text{ha}^{-1}$  in extremely disturbed areas. This rapidly increased to  $599 (\pm 55)$  trees  $\text{ha}^{-1}$  and  $578 (\pm 112)$  trees  $\text{ha}^{-1}$  12 and 22 years after windthrow disturbance, respectively. This apparently fast recovery of TPH was also observed for high and moderate windthrow severities. Figure 2b shows the basal area (BA) as a function of windthrow severity and recovery time. Comparing the BA of extremely disturbed forest 2 years following the windthrow event ( $12.46 \pm 4.5$   $\text{m}^2 \text{ha}^{-1}$ ) with that of extremely disturbed forest after 12 years ( $23.52 \pm 4.51$   $\text{m}^2 \text{ha}^{-1}$ ) and 22 years ( $24.46 \pm 5.03$   $\text{m}^2 \text{ha}^{-1}$ ) yields a gradual increase over time. Similar recovery patterns are observed for the high, moderate and low severity categories.

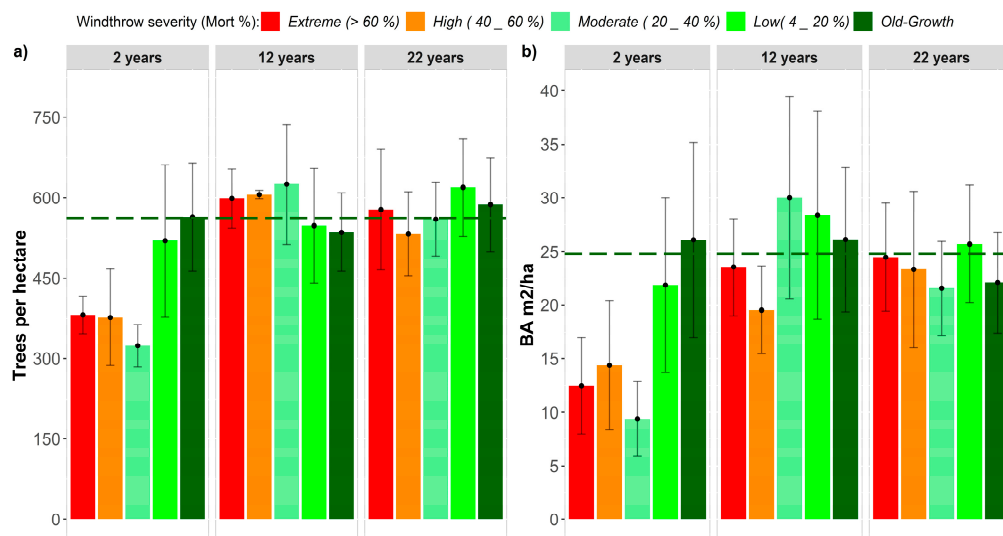


**Figure 2.** Recovery of (a) tree density ( $N \text{ tree ha}^{-1}$ ), and (b) mean basal area ( $\text{m}^2 \text{ha}^{-1}$ ) of old-growth and windthrown forests across the range of severity classes at 2, 12, and 22 years after windthrow. 95% confidence intervals given by the error bars. Dashed dark green lines show the old-growth mean (of the three sites).

#### 3.3.2. Aboveground Tree Biomass

Out of the 4889 trees recorded in our study, 2171 (44.5%) were assigned wood density values at the species level, 1554 (31.7%) at the genus level and 523 (10.7%) at the family level. We did not assign wood density values for 641 (13.1%) trees. We used 95 binned plots distributed over 4 severities and 3 measured years (ranging from 0.09 ha. to 0.12 ha.). Estimates of AGB differed when using Model 1 [37] versus Model 2 [5], mainly due to the relatively higher values given for trees larger than 50 cm DBH by Model 1. However, regardless of which model was used, the overall trajectory of AGB recovery did not change (Appendix B).

Extreme disturbance (>60% mortality) reduced the mean AGB to  $163 \pm 68 \text{ Mg ha}^{-1}$  (2 years after windthrow). AGB increased to  $323.4 \pm 138.7 \text{ Mg ha}^{-1}$  and  $327.5 \pm 86.2 \text{ Mg ha}^{-1}$ , 12 and 22 years after disturbance, respectively. This AGB recovery process was also observed for sites with high severity. Although AGB loss was considerably lower at low and moderate severity, these areas showed an increased biomass compared to old-growth levels 12 years after windthrow. AGB values differed among studied old-growth areas (see details in Appendix C). For these reasons, AGB recovery in disturbed areas was analyzed relative to old-growth values. Thus, a relative sequence of AGB recovery was made (Figure 3A, bottom panel). As suggested by a linear model (Figure 4-Iquitos), AGB stocks at all windthrow severities will recover to ~90% of that observed in contiguous old-growth forest over a time span of 22 years.

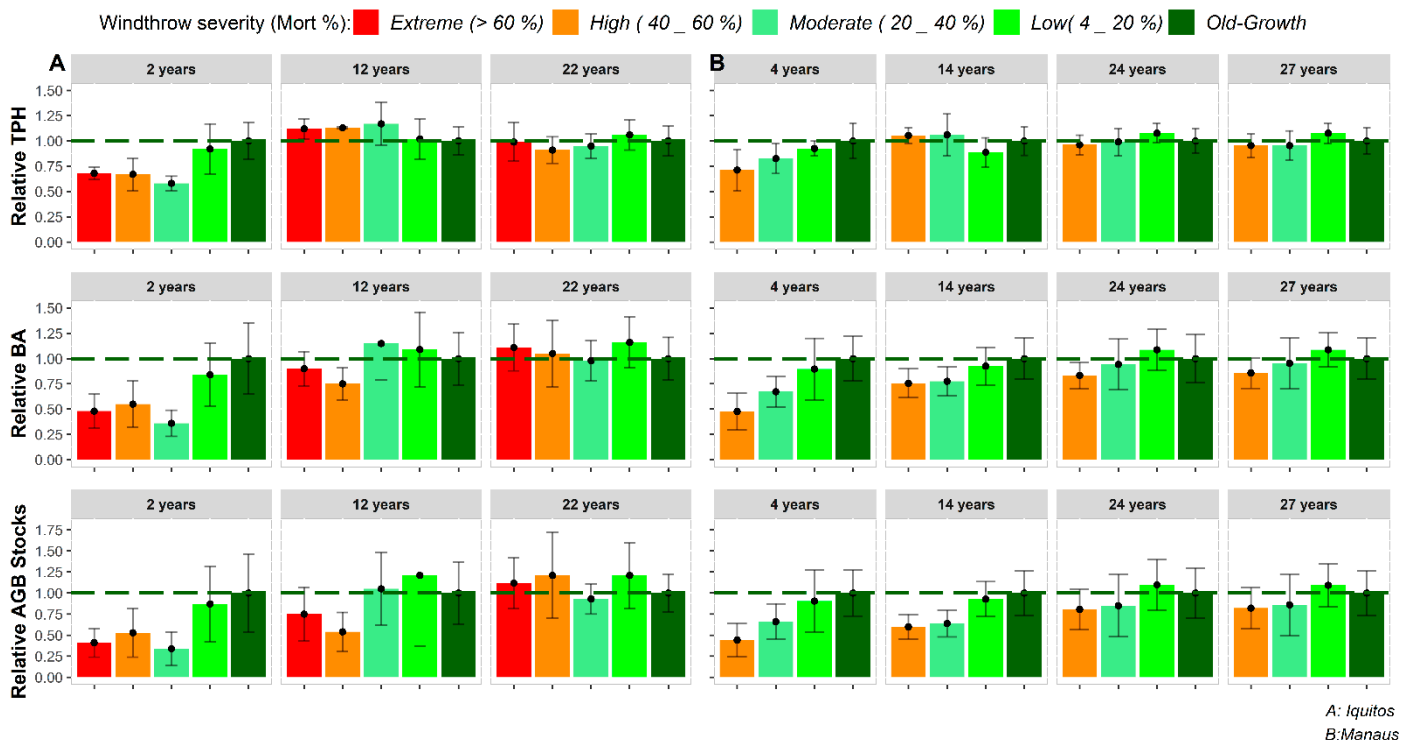


**Figure 3.** Recovery of structural attributes in Northwestern and Central Amazon windthrown forest. Structural attributes: trees per hectare (TPH), basal area (BA) and aboveground biomass (AGB). Sites: (A) Iquitos (NWA) and (B) Manaus (CA). Dashed dark green lines show the old-growth mean and vertical bars the 95% confidence intervals (error bars).



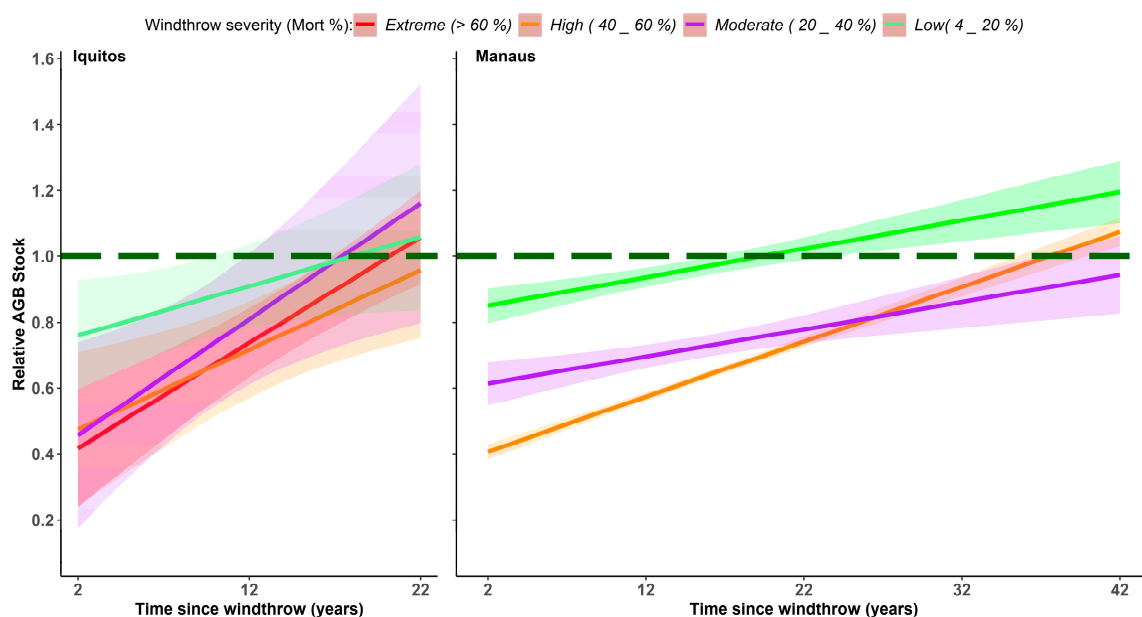


**Figure 4.** Chronosequences (LM CI = 90%) for AGB recovery (>90% Old-growth conditions) across a range of windthrow severities in Iquitos, Peru (Northwestern Amazon) and Manaus, Brazil (Central Amazon). The dashed dark-green line shows the old-growth condition.

## 4. Discussion

### 4.1. Patterns of Recovery after Windthrow

Differences in forest attributes exist across the Amazon Basin [41,42], including tree-mortality predictors [10,43] that can explain different mortality/survival mechanisms when compared across a large region. Winds are an important mechanism of natural disturbance in forests worldwide [44–46]. Windthrows produce varying levels of tree damage/mortality that change forest structure [6,20] and can initiate varying successional trajectories [8,15,28]. Our results give further evidence to the importance of wind as a major disturbance mechanism in Amazon forests [9,12,15,47]

Forest inventories at windthrow sites in the Northwestern Amazon (our plots) and Central Amazon [5,8,15] followed the same overall sampling and analysis design. The degree of windthrow tree mortality estimated from  $\Delta$ NPV was higher (up to 95%) in our Northwestern Amazon sites compared to the Central Amazon (up to 70%) [5,12,15]. For that reason, we included one additional severity class to represent extreme windthrow tree-mortality (>60%).

The  $562 \pm 87$  trees  $\text{ha}^{-1}$  in our old-growth forests is similar to the number reported by other studies conducted in the Northwestern Amazon, for example  $608\text{--}616$  trees  $\text{ha}^{-1}$  [48],  $559 \pm 74$  trees  $\text{ha}^{-1}$  [41],  $589 \pm 20$  trees  $\text{ha}^{-1}$  [49], as well as in the Central Amazon ( $583 \pm 46$  trees  $\text{ha}^{-1}$ ) [15]. Our data on stem density (Figure 3A, top panel) shows that 12 years after windthrow, the windthrown forest reaches the same values observed in the adjacent/contiguous old-growth, and maintains this pattern at least until 22 years of recovery. Compared to plots in the Central Amazon, (Figure 3B, top panel) the patterns of forest recovery are similar in terms of TPH and the time required to recover to old-growth values for both regions is between 12 and 14 years, independent of the severity. Tree density was smaller in the Northwestern Amazon indicating that, for a given windthrow severity, mortality was relatively higher in this region than in the Central Amazon. Tree density recovery following disturbances was also faster in Iquitos (NWA) compared to Manaus (CA). In the Northwestern Amazon, tree density was reduced to  $377 \pm 89$  trees  $\text{ha}^{-1}$  and  $382 \pm 35$  trees  $\text{ha}^{-1}$  2 years after windthrow disturbance in the >40% and > 60% tree-mortality categories, respectively. In the Central Amazon, tree density was  $422 \pm 121$  trees  $\text{ha}^{-1}$  4 years after disturbance in the >40% tree-mortality category [15].

Basal area in old-growth forests in the Northwestern Amazon was previously reported as  $\sim 28 \text{ m}^2 \text{ ha}^{-1}$  [41] and  $27.65 (\pm 2.0) \text{ m}^2 \text{ ha}^{-1}$  [49]. These values are similar to those found at our study sites in the Northwestern Amazon ( $24.8 \pm 2.3 \text{ m}^2 \text{ ha}^{-1}$ ) and those in the Central Amazon ( $26.8 \pm 2.4 \text{ m}^2 \text{ ha}^{-1}$ ) [15]. In our study, the estimated recovery time for the relative basal area (Figure 3A, middle panel) shows a gradual increase in all the windthrow severities. Compared with the Central Amazon (Figure 3B, top and middle panels), we observed a faster recovery of tree density and basal area in the Northwestern Amazon. This also contributes to a more rapid recovery of biomass [15,50] and may be related to changes in floristic composition and species diversity [15,51].

#### 4.2. Time Span of Biomass Recovery

In tropical forests, the recovery of biomass following disturbance can vary greatly depending on the latitude, type and severity of the disturbance. In secondary forests created by human disturbances (e.g., slash-and-burn, and clear cut), biomass recovery to old-growth conditions can take from 66 [52] to >100 years [31,53–55]. These differences in time reflect, among other factors, the availability of nutrients for regrowth [56]. A hurricane in Puerto Rico reduced biomass by 50% [57]. Moreover, impacts and recovery times for this disturbance depended strongly on the degree of hurricane damage, with biomass recovery taking from 4 to 6 years (F0 damage), and from 50 to 150 years (F3 damage) [58,59]. This pattern was also observed after selective logging in Tapajos, Brazil (Central Amazon). Biomass recovery took  $\sim 13$  years [60] and minimally affected forest carbon and water exchanges [61].

Previous studies in old-growth Amazon forests reported AGB ranging from 303 to  $385 \text{ Mg ha}^{-1}$  [62], 155 to  $425 \text{ Mg ha}^{-1}$  [63] and  $\sim 256 \text{ Mg ha}^{-1}$  [64]. Regional-scale variations in biomass are well documented and likely related to factors such as climate [21,22], soils and nutrient availability, or geomorphological characteristics [23]. The causes of regional variations in vegetation structure across different forest types [64] and the main drivers of tree mortality are not yet fully understood [10]. Our results highlight the importance of large-scale windthrows in shaping forest structure in the Northwestern Amazon.

In the Amazon, windthrow distribution extends from the Northwestern Amazon to the Central Amazon [12], showing a spatial and temporal variability in gap sizes [11,65] and mortality rates [6,8,9,12]. In our study, the estimated time to recover AGB increased slightly with windthrow severity. In our study, the recovery to old-growth levels occurred after 22 years (Figure 3A, bottom panel), whereas in the Central Amazon, 24 years were only enough to recover the old-growth levels of attributes observed in forests exposed to low-severity windthrow, and showed a slower growth increment for moderate and high severities even 27 years after windthrow (Figure 3B, bottom panel).

We described the trajectories of biomass recovery in the Northwestern and Central Amazon using linear models (Figure 4). For the Northwestern Amazon, we estimated recovery to be at least > 90% of the old-growth condition after 14 years, 15 years, 18 years, and 20 years since windthrow for low, moderate, extreme, and high windthrow tree-mortality, respectively. For the Central Amazon we estimated  $\sim 10$  years,  $\sim 30$  years, and  $\sim 37$  years for low, high, and moderate windthrow tree-mortality, respectively (details in Supplementary Material SM1, SM2). Differences in the width of confident intervals between the Northwestern and Central Amazon in Figure 4 reflect the number of binned plots used for each site and the numbers of measured years. In the Central Amazon, more complex models such as the generalized additive model (GAM) were used for estimating how biomass recovered to pre-disturbance levels (from 27 to 40 years, maximum) [8].

Our study indicated a faster recovery of biomass in the Northwestern Amazon than in the Central Amazon, which may be explained by the higher productivity in this region [26], and potentially related geographic variations in community attributes, including larger tree diversity [42] which can influence tree mortality patterns [12]. In addition, high competition in combination with water availability [25,66] promotes high productivity, and species that sacrifice defenses in favor of the competitive advantage obtained by rapid growth and low

wood density may be favored in regions with severe disturbance regimes [43]. Thus, faster recovery could be the result of adaptation to more frequent windthrow disturbance in the Northwestern Amazon [12], which provides supporting evidence for the *growth-defense hypothesis* [67].

Ecologists have long recognized that disturbances and recovery processes overlap in spatial and temporal dimensions [68]. In our study sites, the density and size distribution of trees had returned to old-growth levels only 12 years after windthrow. Furthermore, basal area and biomass recovered to pre-disturbance levels within 20 years of the disturbance. This is ~50% faster than the recovery from windthrows observed in the Central Amazon. Future research on forest recovery from windthrows should include a component of geospatial analysis to help explain individual tree response [8].

## 5. Conclusions

This study demonstrated rapid recovery of tree density, basal area, and AGB in the two decades following windthrow events that caused mortality rates >60% in forests near Iquitos, Peru. The observed recovery rates are nearly twice as fast as those reported for a comparable study conducted in the slower-growing forests of the Central Amazon. The variations in forest damage and the recovery dynamics across this geographical and climatic gradient emphasize the effect that extreme wind and rain associated with convective storms can have on the spatial variability of forest structure across the Amazon Basin.

**Supplementary Materials:** The following are available online at <https://www.mdpi.com/article/10.3390/f12060667/s1>, Html SM1: Chronosequences (LM CI = 90%) for AGB recovery (>90% Old-growth conditions) across a range of windthrow severities in Iquitos, Peru (Northwestern Amazon), Html SM2: Chronosequences (LM CI = 90%) for AGB recovery (>90% Old-growth conditions) across a range of windthrow severities in Manaus, Brazil (Central Amazon).

**Author Contributions:** J.D.U.M., D.M.M., R.I.N.-J., J.Q.C., A.B. and S.E.T. performed the research and designed the analysis. J.D.U.M., D.M.M., R.I.N.-J., S.W.R., R.T.-E., W.A.-M., J.D.U.M. performed the data collection. J.D.U.M. analyzed the data and wrote the paper with contributions from R.I.N.-J., S.E.T., D.M.M., A.B., T.P.-G., H.S.J., S.W.R. All authors have read and agreed to the published version of the manuscript.

**Funding:** This research was supported by the Max Planck Institute of Biogeochemistry and the DAAD (German Academic Exchange Service). The field campaign was supported as part of the Next Generation Ecosystem Experiments-Tropics funded by the U.S. Department of Energy, Office of Science, and Office of Biological and Environmental Research. Data collection was supported by NASA Biodiversity (Grant number: NNX09AK21G). The Brazilian data applied in this study is part of the ATTO Project, funded by the German Federal Ministry of Education and Research (BMBF contracts 01LB1001A and 01LK1602A) and the Brazilian Ministério da Ciência, Tecnologia e Inovação (MCTI/FINEP contract 01.11.01248.00) as well as the Max Planck Society (MPG). Brazilian sites are also supported by the *Instituto Nacional de Ciência e Tecnologia INCT-Madeiras da Amazônia*. D.M.M. is also supported by the ATTO Project. R.N.J. is also supported by Reducing Uncertainties in Biogeochemical Interactions through Synthesis and Computation Scientific Focus Area (RUBISCO SFA) under contract to LBNL, which is sponsored by the Regional and Global Climate Modeling (RGCM) Program in the Climate and Environmental Sciences Division (CESD) of the Office of Biological and Environmental Research (BER) in the US Department of Energy Office of Science.

**Institutional Review Board Statement:** Not applicable.

**Informed Consent Statement:** Not applicable.

**Data Availability Statement:** The data presented in this study can be made available upon request from the corresponding author.

**Acknowledgments:** We thank crew members at the National University of the Peruvian Amazon (UNAP), for their logistic support through the project-Muro Huayra (RD N° 321-2009-FCF-UNAP, RR N°1389-2010-UNAP), Jarli Isuiza, Pablo Marin, and Victor Casanova for their dedicated field work.

**Conflicts of Interest:** The authors declare no conflict of interest.

## Appendix A

**Table A1.** Summary of forest floristics characteristic by severity and years after windthrows.

Years after Windthrow	Severity	Number of Families	Number of Genus	Number of Species
2	Extreme	29	52	75
	High	20	42	68
	Moderate	23	45	76
	Low	39	80	174
	Old-growth	46	112	245
12	Extreme	34	86	125
	High	26	53	79
	Moderate	41	95	161
	Low	46	100	185
	Old-growth	52	159	342
22	Extreme	39	112	222
	High	39	84	155
	Moderate	31	54	82
	Low	34	89	170
	Old-growth	47	120	257

## Appendix B

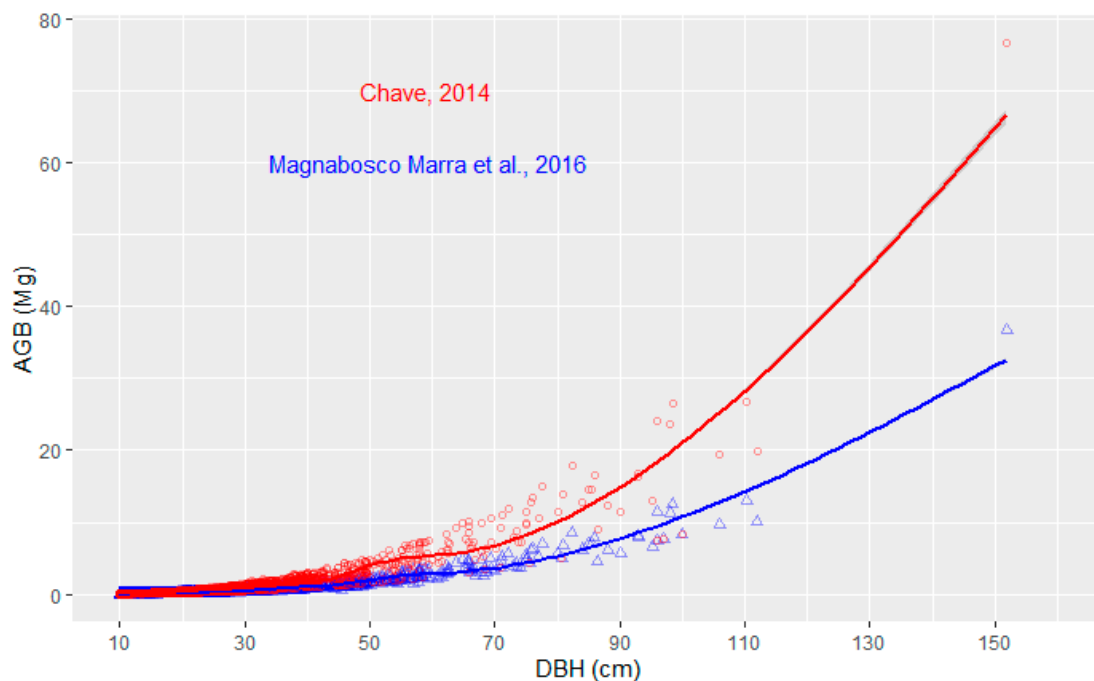


**Figure A1.** AGB estimations for model 1 (Chave et al, 2014) and model 2 (Magnabosco Marra et al., 2016) at circles and triangles, respectively. Red and Blue lines show the regression using Generalized additive model (GAM) for both models.

## Appendix C

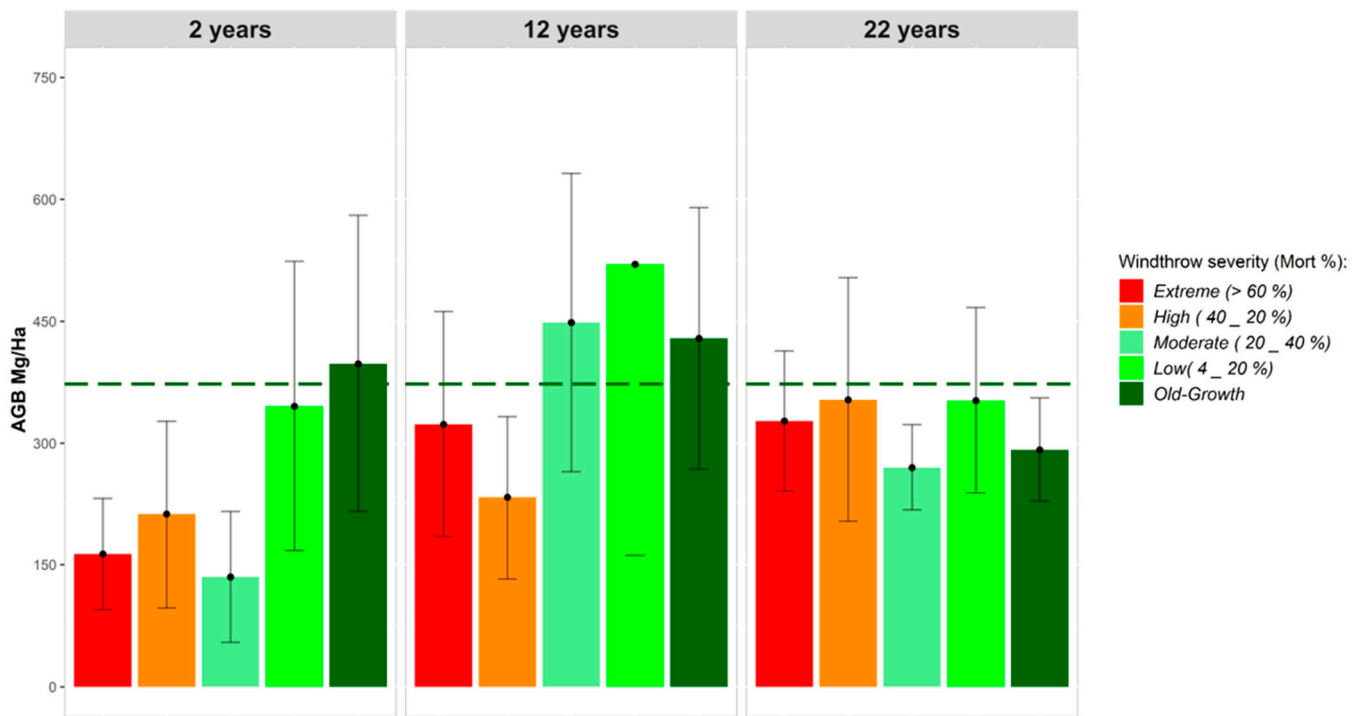


**Figure A2.** Recovery of AGB (Mg ha<sup>-1</sup>) of old-growth and windthrown forests across the range of severity classes at 2, 12, and 22 years after windthrow. 95% confidence intervals given by the error bars. Dashed dark green lines show the old-growth mean (of the three sites).

## References

- Nelson, B.; Amaral, I. Destructive Wind Effects Detected in TM Image in the Amazon Basin. In Proceedings of the International Society for Photogrammetry and Remote Sensing, Rio de Janeiro, Brazil, 26–30 September 1994; Brazil's National Institute for Space Research: Rio de Janeiro, Brazil, 1994; pp. 339–343.
- Garstang, M.; White, S.; Shugart, H.H.; Halverson, J. Convective Cloud Downdrafts as the Cause of Large Blowdowns in the Amazon Rainforest. *Meteorol. Atmos. Phys.* **1998**, *67*, 199–212. [\[CrossRef\]](#)
- Negrón-Juárez, R.I.; Chambers, J.Q.; Guimaraes, G.; Zeng, H.; Raupp, C.F.M.; Marra, D.M.; Ribeiro, G.H.P.M.; Saatchi, S.S.; Nelson, B.W.; Higuchi, N. Widespread Amazon Forest Tree Mortality from a Single Cross-Basin Squall Line Event: Wind-Driven Tree Mortality in Amazonia. *Geophys. Res. Lett.* **2010**, *37*. [\[CrossRef\]](#)
- Mitchell, S.J. Wind as a Natural Disturbance Agent in Forests: A Synthesis. *Forestry* **2013**, *86*, 147–157. [\[CrossRef\]](#)
- Magnabosco Marra, D.; Higuchi, N.; Trumbore, S.E.; Ribeiro, G.H.P.M.; dos Santos, J.; Carneiro, V.M.C.; Lima, A.J.N.; Chambers, J.Q.; Negrón-Juárez, R.I.; Holzwarth, F.; et al. Predicting Biomass of Hyperdiverse and Structurally Complex Central Amazonian Forests—a Virtual Approach Using Extensive Field Data. *Biogeosciences* **2016**, *13*, 1553–1570. [\[CrossRef\]](#)
- Rifai, S.W.; Urquiza Muñoz, J.D.; Negrón-Juárez, R.I.; Ramírez Arévalo, F.R.; Tello-Espinoza, R.; Vanderwel, M.C.; Lichstein, J.W.; Chambers, J.Q.; Bohlman, S.A. Landscape-Scale Consequences of Differential Tree Mortality from Catastrophic Wind Disturbance in the Amazon. *Ecol. Appl.* **2016**, *26*, 2225–2237. [\[CrossRef\]](#)
- Negrón-Juárez, R.; Jenkins, H.; Raupp, C.; Riley, W.; Kueppers, L.; Magnabosco Marra, D.; Ribeiro, G.; Monteiro, M.; Candido, L.; Chambers, J.; et al. Windthrow Variability in Central Amazonia. *Atmosphere* **2017**, *8*, 28. [\[CrossRef\]](#)
- Magnabosco Marra, D.; Trumbore, S.E.; Higuchi, N.; Ribeiro, G.H.P.M.; Negrón-Juárez, R.I.; Holzwarth, F.; Rifai, S.W.; dos Santos, J.; Lima, A.J.N.; Kinupp, V.F.; et al. Windthrows Control Biomass Patterns and Functional Composition of Amazon Forests. *Glob. Chang. Biol.* **2018**, *24*, 5867–5881. [\[CrossRef\]](#)
- Silvério, D.V.; Brando, P.M.; Bustamante, M.M.C.; Putz, F.E.; Marra, D.M.; Levick, S.R.; Trumbore, S.E. Fire, Fragmentation, and Windstorms: A Recipe for Tropical Forest Degradation. *J. Ecol.* **2019**, *107*, 656–667. [\[CrossRef\]](#)
- Esquivel-Muelbert, A.; Phillips, O.L.; Brien, R.J.W.; Fauset, S.; Sullivan, M.J.P.; Baker, T.R.; Chao, K.-J.; Feldpausch, T.R.; Gloor, E.; Higuchi, N.; et al. Tree Mode of Death and Mortality Risk Factors across Amazon Forests. *Nat. Commun.* **2020**, *11*, 5515. [\[CrossRef\]](#)
- Espírito-Santo, F.D.B.; Gloor, M.; Keller, M.; Malhi, Y.; Saatchi, S.; Nelson, B.; Junior, R.C.O.; Pereira, C.; Lloyd, J.; Frothingham, S.; et al. Size and Frequency of Natural Forest Disturbances and the Amazon Forest Carbon Balance. *Nat. Commun.* **2014**, *5*, 3434. [\[CrossRef\]](#)



12. Negrón-Juárez, R.I.; Holm, J.A.; Marra, D.M.; Rifai, S.W.; Riley, W.J.; Chambers, J.Q.; Koven, C.D.; Knox, R.G.; McGroddy, M.E.; Di Vittorio, A.V.; et al. Vulnerability of Amazon Forests to Storm-Driven Tree Mortality. *Environ. Res. Lett.* **2018**, *13*, 054021. [[CrossRef](#)]
13. Chesson, P. Overview: Nonequilibrium community theories: Chance, variability, history, and coexistence. In *Community Ecology*; Diamond, J., Case, T.J., Eds.; Harper and Row: New York, NY, USA, 1986; pp. 229–239.
14. Ennos, A.R. Wind as a Ecological Factor. *Trends Ecol. Evol.* **1997**, *12*, 108–111. [[CrossRef](#)]
15. Marra, D.M.; Chambers, J.Q.; Higuchi, N.; Trumbore, S.E.; Ribeiro, G.H.P.M.; dos Santos, J.; Negrón-Juárez, R.I.; Reu, B.; Wirth, C. Large-Scale Wind Disturbances Promote Tree Diversity in a Central Amazon Forest. *PLoS ONE* **2014**, *9*, e103711. [[CrossRef](#)]
16. Ulanova, N.G. The Effects of Windthrow on Forests at Different Spatial Scales: A Review. *For. Ecol. Manag.* **2000**, *135*, 155–167. [[CrossRef](#)]
17. Denslow, J.S. Tropical Rainforest Gaps and Tree Species Diversity. *Annu. Rev. Ecol. Syst.* **1987**, *18*, 431–451. [[CrossRef](#)]
18. Baker, T.R.; Vela Díaz, D.M.; Chama Moscoso, V.; Navarro, G.; Monteagudo, A.; Pinto, R.; Cangani, K.; Fyllas, N.M.; Lopez Gonzalez, G.; Laurance, W.F.; et al. Consistent, Small Effects of Treefall Disturbances on the Composition and Diversity of Four Amazonian Forests. *J. Ecol.* **2016**, *104*, 497–506. [[CrossRef](#)] [[PubMed](#)]
19. Seidl, R.; Schelhaas, M.-J.; Lexer, M.J. Unraveling the Drivers of Intensifying Forest Disturbance Regimes in Europe: Drivers of Forest Disturbance Intensification. *Glob. Chang. Biol.* **2011**, *17*, 2842–2852. [[CrossRef](#)]
20. Quine, C.P.; Gardiner, B.A. Understanding How the Interaction of Wind and Trees Results in Windthrow, Stem Breakage, and Canopy Gap Formation. In *Plant Disturbance Ecology*; Elsevier: Amsterdam, The Netherlands, 2007; pp. 103–155. ISBN 978-0-12-088778-1.
21. Espinoza Villar, J.C.; Ronchail, J.; Guyot, J.-L.; Cochonneau, G.; Naziano, F.; Lavado, W.; De Oliveira, E.; Pombosa, R.; Vauchel, P. Spatio-Temporal Rainfall Variability in the Amazon Basin Countries (Brazil, Peru, Bolivia, Colombia, and Ecuador). *Int. J. Climatol.* **2009**, *29*, 1574–1594. [[CrossRef](#)]
22. Marengo, J.A. Interdecadal Variability and Trends of Rainfall across the Amazon Basin. *Theor. Appl. Climatol.* **2004**, *78*, 79–96. [[CrossRef](#)]
23. Quesada, C.A.; Lloyd, J.; Anderson, L.O.; Fyllas, N.M.; Schwarz, M.; Czimczik, C.I. Soils of Amazonia with Particular Reference to the Rainfor Sites. *Biogeosciences* **2011**, *8*, 1415–1440. [[CrossRef](#)]
24. Gloor, M.; Brienen, R.J.W.; Galbraith, D.; Feldpausch, T.R.; Schöngart, J.; Guyot, J.-L.; Espinoza, J.C.; Lloyd, J.; Phillips, O.L. Intensification of the Amazon Hydrological Cycle over the Last Two Decades. *Geophys. Res. Lett.* **2013**, *40*, 1729–1733. [[CrossRef](#)]
25. Nemani, R.R. Climate-Driven Increases in Global Terrestrial Net Primary Production from 1982 to 1999. *Science* **2003**, *300*, 1560–1563. [[CrossRef](#)] [[PubMed](#)]
26. Malhi, Y.; Davidson, E.A. Biogeochemistry and Ecology of terrestrial Ecosystems of Amazonia. In *Amazonia and Global Change*; American Geophysical Union: Washington, DC, USA, 2009; ISBN 978-0-87590-476-4.
27. de Mello Ribeiro, G.H.P.; Suwa, R.; Marra, D.M.; Lima, A.J.N.; Kajimoto, T.; Ishizuka, M.; Higuchi, N. Allometry for Juvenile Trees in an Amazonian Forest after Wind Disturbance. *JARQ* **2014**, *48*, 213–219. [[CrossRef](#)]
28. Andrews, T.; Dietze, M.; Booth, R. Climate or Disturbance: Temperate Forest Structural Change and Carbon Sink Potential. *bioRxiv* **2018**, 478693. [[CrossRef](#)]
29. Sombroek, W. Spatial and Temporal Patterns of Amazon Rainfall: Consequences for the Planning of Agricultural Occupation and the Protection of Primary Forests. *AMBIO J. Hum. Environ.* **2001**, *30*, 388–396. [[CrossRef](#)] [[PubMed](#)]
30. Adams, J.B.; Gillespie, A.R. *Remote Sensing of Landscapes with Spectral Images: A Physical Modeling Approach*; Cambridge University Press: Cambridge, UK, 2006; ISBN 978-0-511-61719-5.
31. Saldarriaga, J.G.; West, D.C.; Sharp, M.L.; Uhl, C. Long-Term Chronosequence of Forest Succession in the Upper Rio Negro of Colombia and Venezuela. *J. Ecol.* **1988**, *76*, 938. [[CrossRef](#)]
32. Masek, J.G.; Vermote, E.F.; Saleous, N.E.; Wolfe, R.; Hall, F.G.; Huemmrich, K.F.; Gao, F.; Kutler, J.; Lim, T.-K. A Landsat Surface Reflectance Dataset for North America, 1990–2000. *IEEE Geosci. Remote Sens. Lett.* **2006**, *3*, 68–72. [[CrossRef](#)]
33. Gorelick, N.; Hancher, M.; Dixon, M.; Ilyushchenko, S.; Thau, D.; Moore, R. Google Earth Engine: Planetary-Scale Geospatial Analysis for Everyone. *Remote Sens. Environ.* **2017**, *202*, 18–27. [[CrossRef](#)]
34. Adams, J. Classification of Multispectral Images Based on Fractions of Endmembers: Application to Land-Cover Change in the Brazilian Amazon. *Remote Sens. Environ.* **1995**, *52*, 137–154. [[CrossRef](#)]
35. Chambers, J.Q.; Negrón-Juárez, R.I.; Hurr, G.C.; Marra, D.M.; Higuchi, N. Lack of Intermediate-Scale Disturbance Data Prevents Robust Extrapolation of Plot-Level Tree Mortality Rates for Old-Growth Tropical Forests: Clustered Gaps Tropical Tree Mortality Rates. *Ecol. Lett.* **2009**, *12*, E22–E25. [[CrossRef](#)]
36. Balderas Torres, A.; Lovett, J.C. Using Basal Area to Estimate Aboveground Carbon Stocks in Forests: La Primavera Biosphere’s Reserve, Mexico. *Forestry* **2013**, *86*, 267–281. [[CrossRef](#)]
37. Chave, J.; Réjou-Méchain, M.; Búrquez, A.; Chidumayo, E.; Colgan, M.S.; Delitti, W.B.C.; Duque, A.; Eid, T.; Fearnside, P.M.; Goodman, R.C.; et al. Improved Allometric Models to Estimate the Aboveground Biomass of Tropical Trees. *Glob. Chang. Biol.* **2014**, *20*, 3177–3190. [[CrossRef](#)] [[PubMed](#)]
38. Chave, J.; Coomes, D.; Jansen, S.; Lewis, S.L.; Swenson, N.G.; Zanne, A.E. Towards a Worldwide Wood Economics Spectrum. *Ecol. Lett.* **2009**, *12*, 351–366. [[CrossRef](#)]

39. De Oliveira, M.M.; Higuchi, N.; Celes, C.H.; Higuchi, F.G. Tamanho e Formas de Parcelas Para Inventários Florestais de Espécies Arbóreas na Amazônia Central. *Ciênc. Florest.* **2014**, *24*, 645–653. [[CrossRef](#)]
40. R Core Team. *R: A Language and Environment for Statistical Computing*; R Foundation for Statistical Computing: Vienna, Austria, 2013.
41. Feldpausch, T.R.; Banin, L.; Phillips, O.L.; Baker, T.R.; Lewis, S.L.; Quesada, C.A.; Affum-Baffoe, K.; Arets, E.J.M.M.; Berry, N.J.; Bird, M.; et al. Height-Diameter Allometry of Tropical Forest Trees. *Biogeosciences* **2011**, *8*, 1081–1106. [[CrossRef](#)]
42. ter Steege, H.; Pitman, N.C.A.; Phillips, O.L.; Chave, J.; Sabatier, D.; Duque, A.; Molino, J.-F.; Prévost, M.-F.; Spichiger, R.; Castellanos, H.; et al. Continental-Scale Patterns of Canopy Tree Composition and Function across Amazonia. *Nature* **2006**, *443*, 444–447. [[CrossRef](#)]
43. Chao, K.-J.; Phillips, O.L.; Gloor, E.; Monteagudo, A.; Torres-Lezama, A.; Martínez, R.V. Growth and Wood Density Predict Tree Mortality in Amazon Forests. *J. Ecol.* **2008**, *96*, 281–292. [[CrossRef](#)]
44. Aigbe, H.I.; Omokhua, G.E. Modeling Diameter Distribution of the Tropical Rainforest in Oban Forest Reserve. *JEE* **2014**, *5*, 130. [[CrossRef](#)]
45. Muller-Landau, H.C.; Condit, R.S.; Harms, K.E.; Marks, C.O.; Thomas, S.C.; Bunyavejchewin, S.; Chuyong, G.; Co, L.; Davies, S.; Foster, R.; et al. Comparing Tropical Forest Tree Size Distributions with the Predictions of Metabolic Ecology and Equilibrium Models. *Ecol. Lett.* **2006**, *9*, 589–602. [[CrossRef](#)]
46. Niklas, K.J.; Midgley, J.J.; Rand, R.H. Tree Size Frequency Distributions, Plant Density, Age and Community Disturbance: Tree Size Distributions. *Ecol. Lett.* **2003**, *6*, 405–411. [[CrossRef](#)]
47. Chambers, J.Q.; Negron-Juarez, R.I.; Marra, D.M.; Di Vittorio, A.; Tews, J.; Roberts, D.; Ribeiro, G.H.P.M.; Trumbore, S.E.; Higuchi, N. The Steady-State Mosaic of Disturbance and Succession across an Old-Growth Central Amazon Forest Landscape. *Proc. Natl. Acad. Sci. USA* **2013**, *110*, 3949–3954. [[CrossRef](#)] [[PubMed](#)]
48. Martinez, R.V.; Phillips, O.L. Allpahuayo: Floristics, Structure, and Dynamics of a High-Diversity Forest in Amazonian Peru. *Ann. Mo. Bot. Gard.* **2000**, *87*, 499. [[CrossRef](#)]
49. Lewis, S.L.; Phillips, O.L.; Baker, T.R.; Lloyd, J.; Malhi, Y.; Almeida, S.; Higuchi, N.; Laurance, W.F.; Neill, D.A.; Silva, J.N.M.; et al. Concerted Changes in Tropical Forest Structure and Dynamics: Evidence from 50 South American Long-Term Plots. *Phil. Trans. R. Soc. Lond. B* **2004**, *359*, 421–436. [[CrossRef](#)] [[PubMed](#)]
50. Chazdon, R.L.; Letcher, S.G.; van Breugel, M.; Martínez-Ramos, M.; Bongers, F.; Finegan, B. Rates of Change in Tree Communities of Secondary Neotropical Forests Following Major Disturbances. *Phil. Trans. R. Soc. B* **2007**, *362*, 273–289. [[CrossRef](#)]
51. Sheil, D.; Burslem, D.F.R.P. Disturbing Hypotheses in Tropical Forests. *Trends Ecol. Evol.* **2003**, *18*, 18–26. [[CrossRef](#)]
52. Poorter, L.; Bongers, F.; Aide, T.M.; Almeyda Zambrano, A.M.; Balvanera, P.; Becknell, J.M.; Boukili, V.; Brancalion, P.H.S.; Broadbent, E.N.; Chazdon, R.L.; et al. Biomass Resilience of Neotropical Secondary Forests. *Nature* **2016**, *530*, 211–214. [[CrossRef](#)]
53. Chazdon, R.L. Tropical Forest Recovery: Legacies of Human Impact and Natural Disturbances. *Perspect. Plant Ecol. Evol. Syst.* **2003**, *6*, 51–71. [[CrossRef](#)]
54. D'Oliveira, M.V.N.; Alvarado, E.C.; Santos, J.C.; Carvalho, J.A. Forest Natural Regeneration and Biomass Production after Slash and Burn in a Seasonally Dry Forest in the Southern Brazilian Amazon. *For. Ecol. Manag.* **2011**, *261*, 1490–1498. [[CrossRef](#)]
55. Elias, F.; Ferreira, J.; Lennox, G.D.; Berenguer, E.; Ferreira, S.; Schwartz, G.; de Oliveira Melo, L.; Reis Júnior, D.N.; Nascimento, R.O.; Ferreira, F.N.; et al. Assessing the Growth and Climate Sensitivity of Secondary Forests in Highly Deforested Amazonian Landscapes. *Ecology* **2020**, *101*. [[CrossRef](#)]
56. Veldkamp, E.; Schmidt, M.; Powers, J.S.; Corre, M.D. Deforestation and Reforestation Impacts on Soils in the Tropics. *Nature Rev. Earth Environ.* **2020**, *1*, 590–605. [[CrossRef](#)]
57. Scatena, F.N.; Moya, S.; Estrada, C.; China, J.D. The First Five Years in the Reorganization of Aboveground Biomass and Nutrient Use Following Hurricane Hugo in the Bisley Experimental Watersheds, Luquillo Experimental Forest, Puerto Rico. *Biotropica* **1996**, *28*, 424. [[CrossRef](#)]
58. Everham, E.M.; Brokaw, N.V.L. Forest Damage and Recovery from Catastrophic Wind. *Bot. Rev.* **1996**, *62*, 113–185. [[CrossRef](#)]
59. Boose, E.R.; Serrano, M.I.; Foster, D.R. Landscape and Regional Impacts of Hurricanes in Puerto Rico. *Ecol. Monogr.* **2004**, *74*, 335–352. [[CrossRef](#)]
60. Silva, J.N.M.; de Carvalho, J.O.P.; Lopes, J.d.C.A.; de Almeida, B.F.; Costa, D.H.M.; de Oliveira, L.C.; Vanclay, J.K.; Skovsgaard, J.P. Growth and Yield of a Tropical Rain Forest in the Brazilian Amazon 13 Years after Logging. *For. Ecol. Manag.* **1995**, *71*, 267–274. [[CrossRef](#)]
61. Miller, S.D.; Goulden, M.L.; Huttyra, L.R.; Keller, M.; Saleska, S.R.; Wofsy, S.C.; Figueira, A.M.S.; da Rocha, H.R.; de Camargo, P.B. Reduced Impact Logging Minimally Alters Tropical Rainforest Carbon and Energy Exchange. *Proc. Natl. Acad. Sci. USA* **2011**, *108*, 19431–19435. [[CrossRef](#)] [[PubMed](#)]
62. Nogueira, E.M.; Fearnside, P.M.; Nelson, B.W.; Barbosa, R.I.; Keizer, E.W.H. Estimates of Forest Biomass in the Brazilian Amazon: New Allometric Equations and Adjustments to Biomass from Wood-Volume Inventories. *For. Ecol. Manag.* **2008**, *256*, 1853–1867. [[CrossRef](#)]
63. Houghton, R.A.; Lawrence, K.T.; Hackler, J.L.; Brown, S. The Spatial Distribution of Forest Biomass in the Brazilian Amazon: A Comparison of Estimates. *Glob. Chang. Biol.* **2001**, *7*, 731–746. [[CrossRef](#)]
64. Lima, A.J.N.; Suwa, R.; de Mello Ribeiro, G.H.P.; Kajimoto, T.; dos Santos, J.; da Silva, R.P.; de Souza, C.A.S.; de Barros, P.C.; Noguchi, H.; Ishizuka, M.; et al. Allometric Models for Estimating Above- and below-Ground Biomass in Amazonian Forests at São Gabriel Da Cachoeira in the Upper Rio Negro, Brazil. *For. Ecol. Manag.* **2012**, *277*, 163–172. [[CrossRef](#)]

65. Espírito, F.D.B.; Keller, M.; Braswell, B.; Nelson, B.W.; Frolking, S.; Vicente, G. Storm Intensity and Old-growth Forest Disturbances in the Amazon Region. *Geophys. Res. Lett.* **2010**, *37*, 6. [[CrossRef](#)]
66. Rozendaal, D.M.A.; Phillips, O.L.; Lewis, S.L.; Affum-Baffoe, K.; Alvarez-Davila, E.; Andrade, A.; Aragão, L.E.O.C.; Araujo-Murakami, A.; Baker, T.R.; Bánki, O.; et al. Competition Influences Tree Growth, but Not Mortality, across Environmental Gradients in Amazonia and Tropical Africa. *Ecology* **2020**, *101*, e03052. [[CrossRef](#)]
67. Stephenson, N.L.; van Mantgem, P.J.; Bunn, A.G.; Bruner, H.; Harmon, M.E.; O'Connell, K.B.; Urban, D.L.; Franklin, J.F. Causes and Implications of the Correlation between Forest Productivity and Tree Mortality Rates. *Ecol. Monogr.* **2011**, *81*, 527–555. [[CrossRef](#)]
68. Zelnik, Y.R.; Arnoldi, J.-F.; Loreau, M. The Impact of Spatial and Temporal Dimensions of Disturbances on Ecosystem Stability. *Front. Ecol. Evol.* **2018**, *6*, 224. [[CrossRef](#)] [[PubMed](#)]